

Analysis and reinterpretation of historical AEM data sets: McArthur Basin, NT

Alan Yusen Ley-Cooper^{1,2}, Tim Munday¹, Tania Ibrahimi¹ and Kevin Cahill¹

Background

This paper presents the preliminary results from the modelling and interpretation of public domain airborne electromagnetic (AEM) datasets covering the eastern part of the McArthur Basin in Australia's Northern Territory. The main purpose of the work is to assess their value for exploration through cover, and in particular, for assisting the mapping of key stratigraphic units in the subsurface when the data is reprocessed using more modern interpretation methods.

The work involved data-mining and the compilation of existing company and NTGS AEM data. The eastern portion of the McArthur Basin has an extensive coverage of data from a range of AEM systems, including helicopter and fixed-wing time-domain systems, plus some local scale helicopter frequency-domain surveys. Of these, only a few have been subject to analysis and interpretation using more recent modelling and inversion methods.

An assessment of these historical AEM data with a focus on the Batten Fault Zone has enabled us to evaluate their suitability for full non-linear inversion, or their transformation using approximate methods, to yield conductivity-depth information. Adequate system characteristics descriptions are required so the data can then be used in the inversion or transformation process. This approach attempts to mitigate the influence of different system parameters and geometry employed in data acquisition. A key objective for the project is to develop a set of modelled results that permit the geographic transfer of geological understanding based on a more consistent spatial model of ground conductivity. Collation and documentation of system and survey characteristics has been critical and forms an integral part of this activity.

Introduction

AEM methods offer an efficient way of investigating the geo-electrical structure of large areas in a timely manner and at relatively low cost. We have reprocessed historic AEM surveys, most of which were acquired by mineral exploration companies and usually originally used as 'bump detectors'. Previous work elsewhere in Australia has demonstrated the value of reprocessing legacy data for mapping geological structures in the near-surface (eg Ley-Cooper and Munday 2013). There is an extensive literature that also demonstrates the added benefit that the inversion process brings to the analysis and understanding of the AEM data from a geological mapping perspective.

The derived AEM models from all of the surveys in the eastern McArthur Basin will be compiled into a single set of maps depicting subsurface conductivity at different depths. The intent is to provide more elements and greater geological information on the spatial distribution, character, and connectivity of subsurface features, as well as provide data on groundwater quality and potentially different materials

in the area. Some of these surveys overlap, but cannot be easily linked or compared seamlessly as they were acquired and processed independently by different companies and/or contractors, and at different times.

The importance of proper system characterisation and modelling

When attempting to extract quantitative models of subsurface conductivity from AEM data, the reliability of the model parameters that are fed into the inversion algorithm become crucial. Inversion algorithms require quality data, precise forward-modelling and reliable systems specifications in order to achieve usable outcomes. These elements are not always available, particularly when dealing with legacy datasets. Most commonly, the limiting factor can be attributed to the absence of adequate information about the system itself, including the waveform of the transmitter, the system geometry and system noise characteristics.

All systems have intrinsic peculiarities which need to be identified and properly defined to reduce the uncertainties in their modelling. Many examples in the literature (ie Christiansen *et al* 2011, Viezzoli *et al* 2013, Ley and Munday 2013) have illustrated the consequence of an inaccurate description of AEM system parameters and how these can compromise the results. In this work, we have looked at over 40 different datasets that have been acquired across the basin between 1992 and 2008.

Airborne EM systems

Airborne EM systems consist of a transmitter (Tx) loop and a receiver coil (Rx) arranged in different geometries which are lifted on a platform. AEM transmitters induce a current into the ground that diffuses downward and outward into the subsurface. Frequency and time domain EM methods differ mostly in the way they remove the effect of the induced primary field (Swift, 1988). In general terms, frequency-domain (FDEM) systems induce sinusoidal fields at different frequencies. Through later processing, the primary and secondary fields are separated by subtracting the difference between the measured and predicted fields. FDEM data is recorded as two components for each frequency - an "In-phase" (IP) and "Out-of-phase" (or Quadrature = Q) component. In contrast, time domain EM (TDEM) systems commonly measure the secondary EM field response in the "off-time". No further removal is needed in absence of the transmitted primary.

McArthur Basin AEM dataset

Datasets currently being reviewed for this work come from different providers and instruments (as summarised in **Table 1** and **Figure 1**). All surveys have been subject to a

¹ CSIRO Mineral Resources, 26 Dick Perry Ave, Kensington WA 6151, Australia

² Email: yusen.ley@csiro.au.

QA\QC process and together they comprise the McArthur Basin dataset. The AEM systems that have been employed across the McArthur Basin include HUMMINGBIRD, DIGHEM (Helicopter frequency domain systems); QUESTEM, GEOTEM, INPUT, TEMPEST (fixed-wing time domain EM systems); VTEM and HoiSTEM (helicopter time domain EM systems). Over 40 000 line km of data have been acquired with the seven different systems mentioned above (**Table 1**). The area covered is approximately 400 km² of the eastern McArthur Basin (**Figure 1**)

Table 1. Line km flown by different AEM systems across the eastern McArthur Basin

AEM system	Line km
DIGHEM	862
GEOTEM	11,168
HOISTEM	331
HUMMINGBIRD	1,930
QUESTEM	19,635
TEMPEST	4,447
VTEM	1,739
Total	40,112

Processing and inversion

All datasets are being processed by one or both of two algorithms that transform raw AEM data into conductivity and depth layer models. These include calculation of conductivity, depth and images (CDI's) using EMFlow (Macnae *et al* 1998), and/or the generation of full 1D Layered Earth inversions using the GA_LEI algorithm [developed by Brodie (2010) and described Costello *et al* (2011)]. By stitching all the inverted 1D models, a conceptual 3D conductivity structure can be built and then be coupled with geological information for interpretation.

In **Figure 2** we illustrate the intent of the study, showing a subset of the AEM data sets and a derived interval conductivity (from a full non-linear inversion of the data) for the central part of the study area. A total of fourteen surveys from two AEM systems – the (TEMPEST (Lane *et al* 2000) and VTEM (Witherly *et al* 2004) systems, were used to generate the map shown. Data from these systems have been identified as being readily amenable to processing and transformation using more recent modelling and inversion algorithms. The interval conductivity image shows a highly conductive (>1S/m) zone in the north-east associated with salt water intrusion along the coastal sediments. Variably conductive parts of the McArthur Basin are also apparent further south. A line of TEMPEST data from a survey in the southern portion of the study area (E-W orientated orange line in **Figure 2**) shows the results from their transformation using EMFlow versus conductivity models derived from the GA-LEI inversion (**Figure 3**).

The top panel (A) in **Figure 3** is an indicator of the level of agreement between measured and modelled data. High values of ϕ_d (above 1) are indicators of locations with either spurious data, or where steeply dipping boundaries have strong 2D and 3D effects on the data that cannot be appropriately resolved with the 1D algorithms we have

used. In panel B, the Z (red) and X (black) component measured by the TEMPEST system is displayed as streamed channels of data. The changes in shapes and amplitude of the channel data are indicators of variations of conductivity along the line. Panel C shows a 30 layer smooth model inversion from the GA-LEI, and below it in Panel D, the results from a fast transform (EMFlow CDI) on the same line of data

Panels C and D (**Figure 3**) show some significant differences that should be noted between the fast transform and the inverted models. At a distance 14 000 and 15 000 m from the start of the flight line on the left, a flat-lying conductor is modelled. Results from the full inversion (**Figure 3**: Panel C) resolve it as a segmented body at different depths, whilst the EMFlow CDI transform (**Figure 3**: Panel D) places it nearer to the surface as a more continuous conductivity structure. The CDI also fails to image the deeper feature (~100 m) imaged by the inversion at 594000mE. Dimensions and geometry are better resolved in the fully inverted model.

System comparison

We have also identified areas with overlapping datasets from different systems. In these coincident locations, we have determined there is a basis for further cross validation of derived EM models. As an example, TEMPEST line L400301 is coincident with GEOTEM Line 1281 (See **Figure 4**). **Figure 5** shows the line in profile from where the surveys overlap. The overlap occurs between 5900042mE and 599968mE.

The datasets are of variable quality, and their evaluation and suitability for further processing is still being determined. In **Figure 5** where there is a coincident TEMPEST and GEOTEM line, we have used the conductivity depth images (from EMFlow) and the raw line channel to cross-correlate the derived conductivity models and assess the data.

From the raw channel data, we can see that the GEOTEM data have much higher amplitudes over this area – suggesting a greater ground response (associated with a higher moment). We can also see that the late time channels in the GEOTEM are not monotonically decaying. Abrupt changes and interruptions are indicators of noise in the late time channels that, when modelled, can introduce artefacts in the derived conductivity models.

The TEMPEST data appears less noisy in the late time channels. The decays behave in a much more undulating manner. These data have the added benefit that two components have been measured, allowing further constraints in the modelling. The data comes from a comparatively low-powered system which implies the penetration is less than that of the GEOTEM. The recovered conductivity sections from both systems are similar in places, and they appear to image similar features in the near surface. However, The GEOTEM images conductive structures at much greater depth, structures that are not apparent in the TEMPEST results. Further work is required to resolve the geological significance of these.

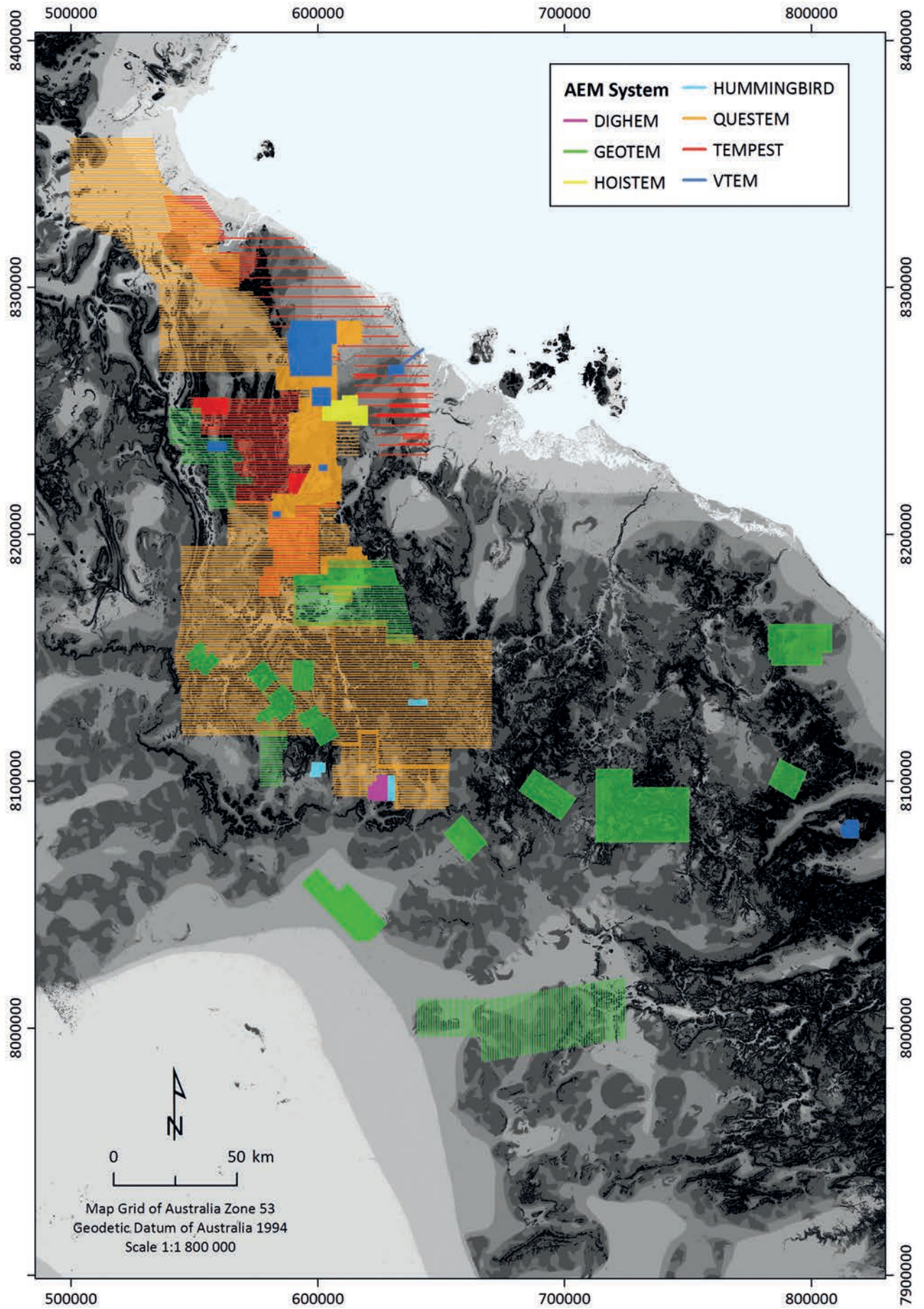


Figure 1. Location map of AEM data sets subject to QA/QC and transformation into an industry standard database format. AEM data sets have been assigned to a system type and flight line orientation. The flight-line distribution of all systems has been draped on a terrane valley bottom flatness index (Gallant and Dowling 2003).

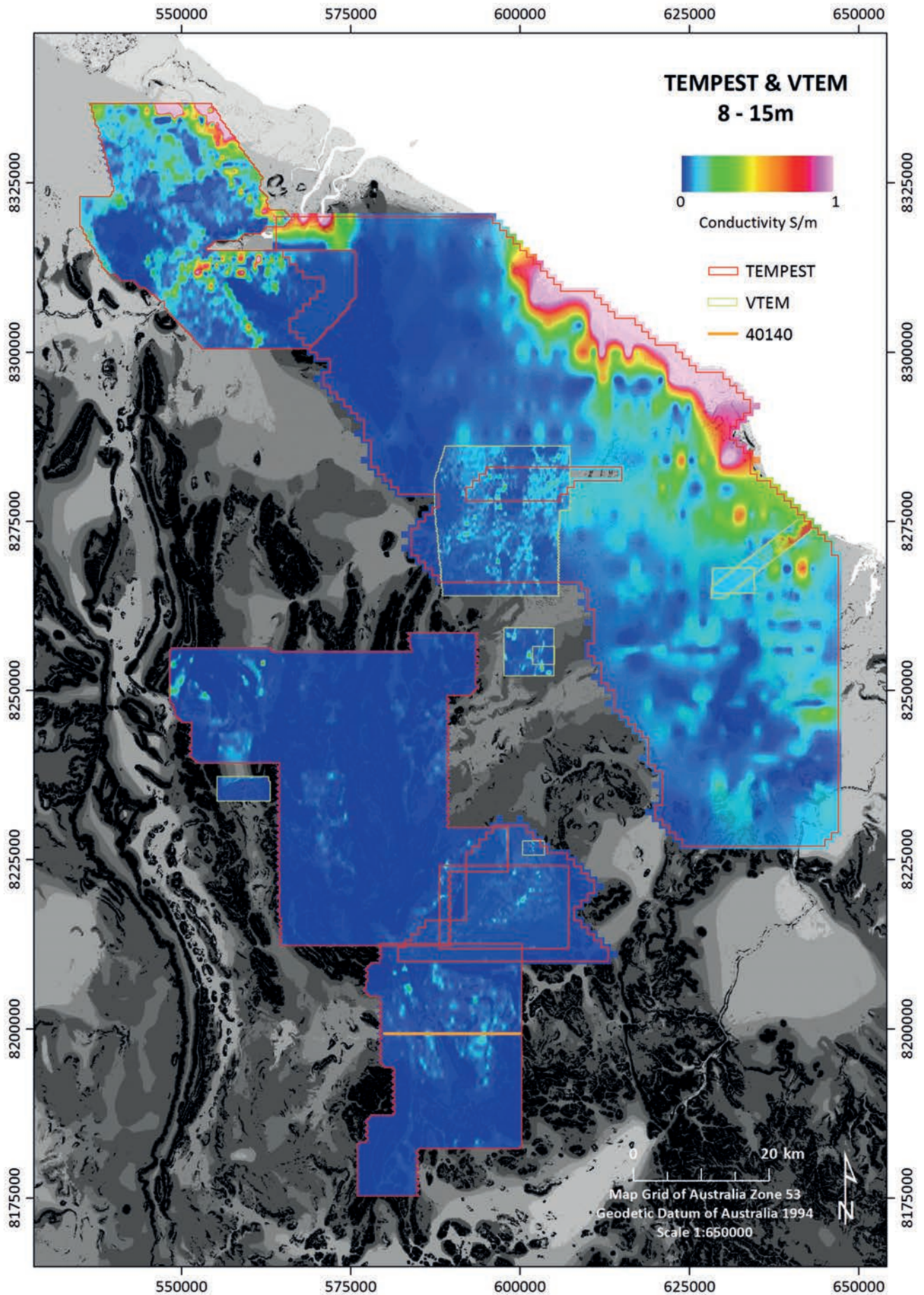


Figure 2. Map of inverted conductivity derived from 14 datasets and 2 different airborne EM systems, at a depth slice range between ~8–15 m below the land surface. Conductivity-depth slice has been draped over a terrane index derived from MrVBF (Valley Bottom Flatness index) processing of the Shuttle SRTM 3 sec DEM.

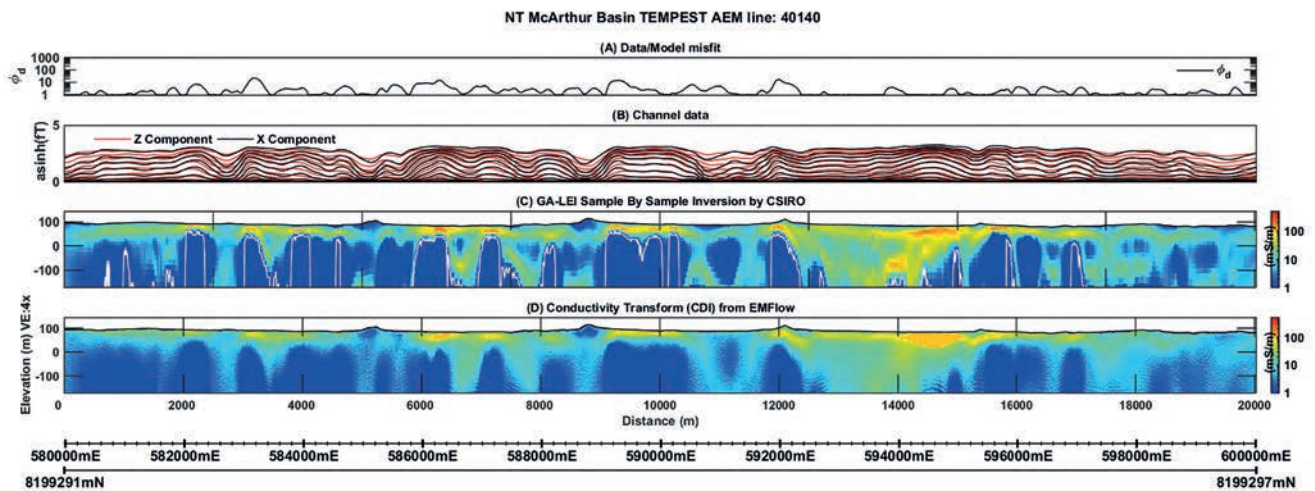


Figure 3. TEMPEST line 40140 showing on the very top panel (A) the level of fit at each location as a profile. In (B) the raw Z and X component channels of EM data displayed as a continuous streamed profile red and black respectively. Bottom two panels (C) and (D) show a comparison between a stitched conductivity-depth transforms (EMFlow) and one from a full non-linear inversion (GA-LEI).

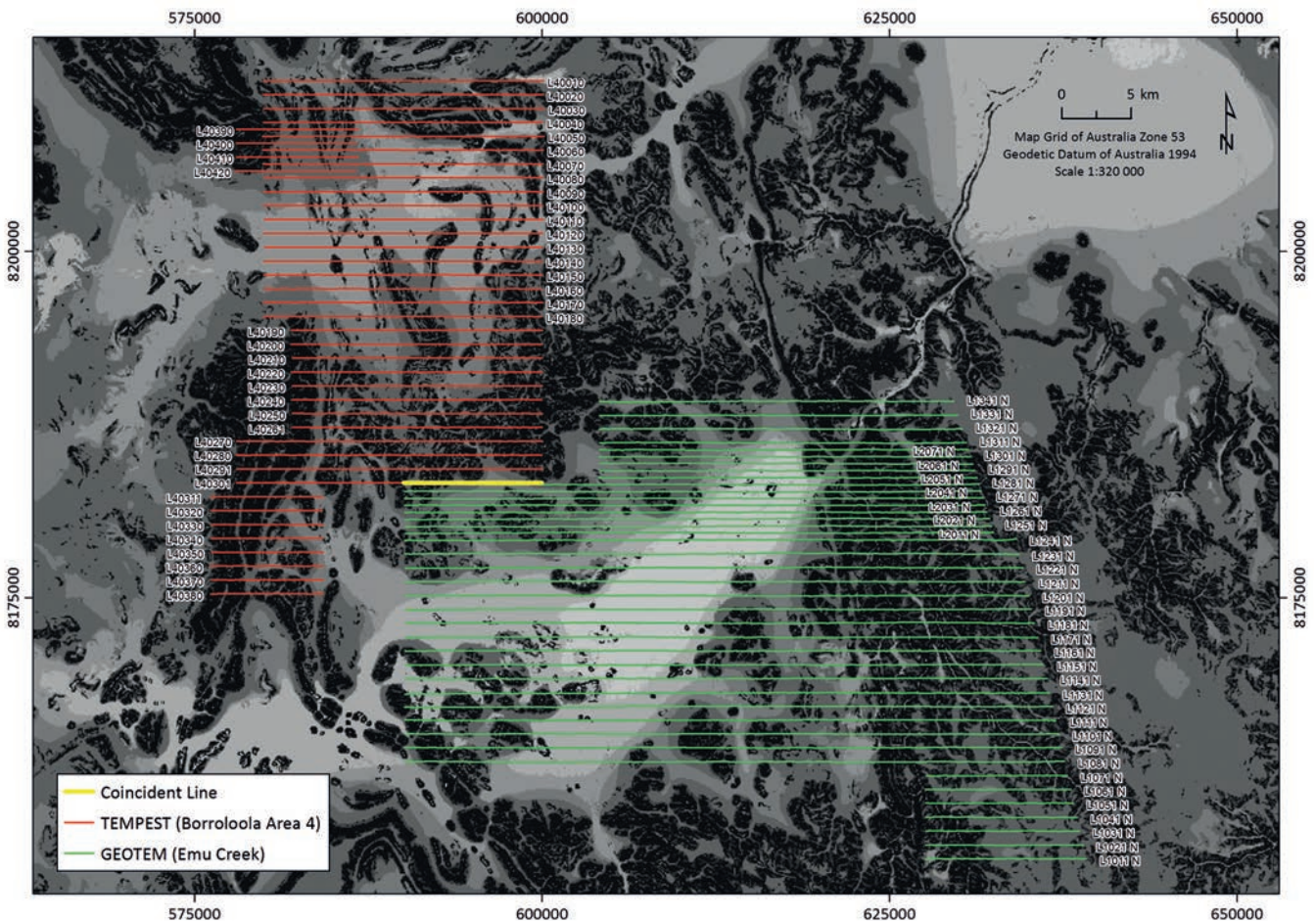


Figure 4. Coincident flight line segment (yellow) with overlapping TEMPEST (red) and a GEOTEM (green) data sets.

Conclusion

Analysis and modelling the available AEM datasets over the McArthur Basin has enabled us to QA/QC and transform legacy data into maps and sections that show the distribution and variations of conductive material at different depths. The available datasets are variable in quality; the absence of detailed metadata on system characteristics and details on survey parameters adds challenges to their combined interpretation.

Direct stratigraphic interpretation of the modelled conductivity structure is possible only if there is a sufficient evidence to show that conductivity change is driven by change in lithology. Geological interpretation at depth will be challenged by the diffuse nature of AEM responses although early results indicate that the conductive response in some of these areas could be driven by particular lithological units.

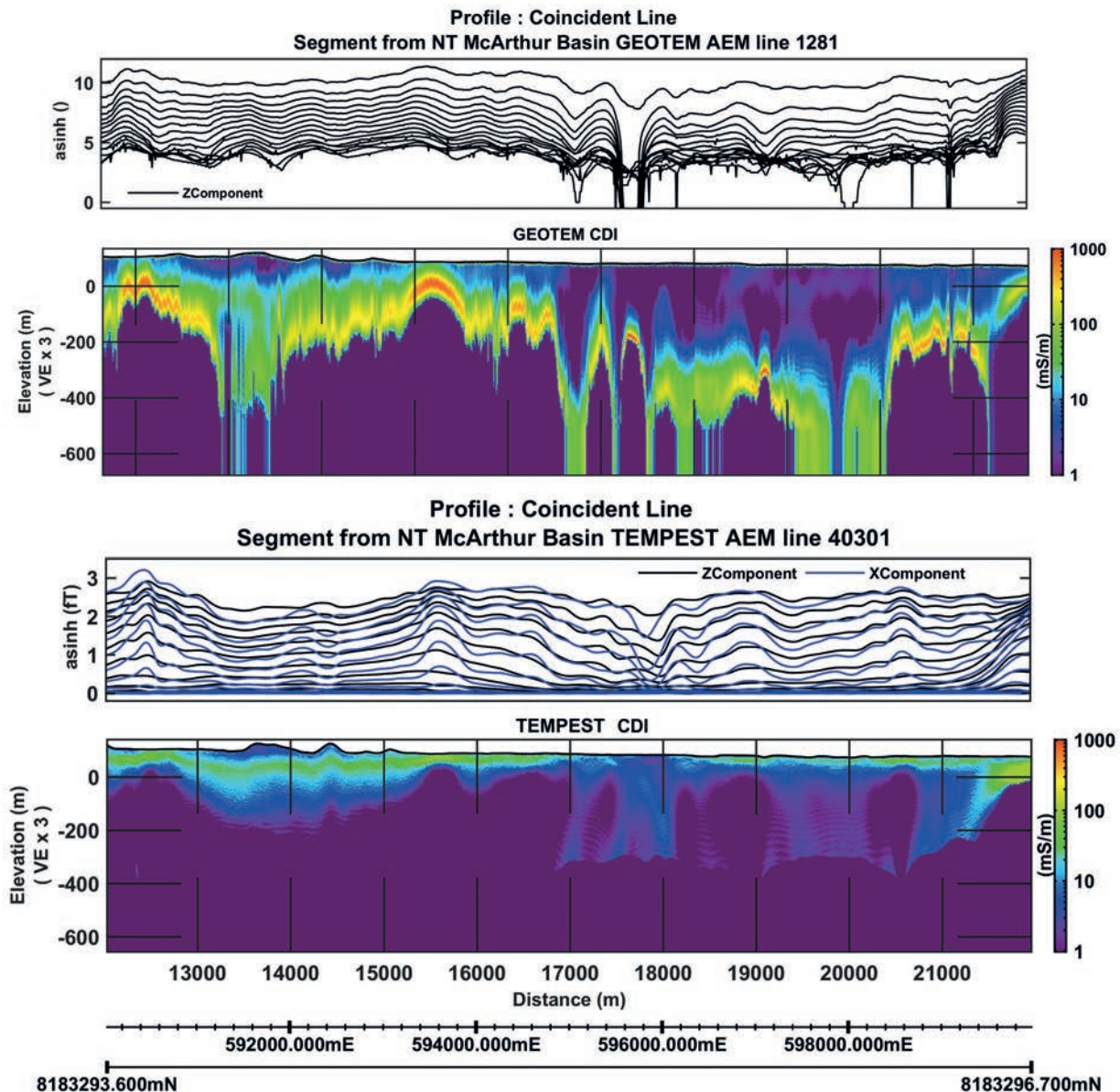


Figure 5. Stitched conductivity depth (EMFlow) profile segment from coincident TEMPEST and GEOTEM flight lines.

References

Brodie RC, 2010. *Holistic Inversion of Airborne Electromagnetic Data*. PhD thesis, The Australian National University, Canberra.

Christiansen AV, Auken E and Viezzoli A, 2011. Quantification of modeling errors in airborne TEM caused by inaccurate system description. *Geophysics* 76(1), F43–F52.

Costello MT, Brodie R and Hutchinson DK, 2011. AEM Geophysics: in Craig MA (editor). ‘*Geological and energy implications of the Pine Creek region airborne electromagnetic (AEM) survey, North Territory, Australia*’. *Geoscience Australia Record* 2011/18, 110–138.

Gallant JC and Dowling TI, 2003. A multiresolution index of valley bottom flatness for mapping depositional areas. *Water Resources Research* 39(12), 1347.

Ley-Cooper AY and Munday TJ, 2013. Groundwater Assessment and Aquifer Characterization in the Musgrave Province, South Australia: Interpretation of SPECTREM Airborne Electromagnetic Data. *Goyder Institute for Water Research Technical Report Series No. 13/7*.

Lane R, Green A, Golding C, Owers M, Pik P, Plunkett C, Sattel D and Thorn B, 2000. An example of 3D conductivity mapping using the TEMPEST airborne electromagnetic system. *Exploration Geophysics* 31, 162–172.

Macnae JC, King A, Stolz N, Osmakoff A and Blaha A, 1998. Fast AEM data processing and inversion. *Exploration Geophysics* 29, 163–169.

Swift CM, 1988. 1. Fundamentals of the Electromagnetic Method: in Nabighian MN, Corbett JD and Society of Exploration Geophysicists (editors). ‘*Electromagnetic Methods in Applied Geophysics*’. *Society of Exploration Geophysics, Tulsa, Okla*, 4-11.

Viezzoli A, Jørgensen F and Sørensen C, 2013. Flawed Processing of Airborne EM Data Affecting Hydrogeological Interpretation. *Groundwater* 51, 191–202.

Witherly K, Irvine D and Morrison E, 2004. *The Geotech VTEM time domain helicopter EM system*. Conference abstracts - ASEG 17th Geophysical Conference and Exhibition, Sydney 2004. Australian Society of Exploration Geophysicists.